S-Oxygenation of Thiocarbamides II: Oxidation of Trimethylthiourea by Chlorite and Chlorine Dioxide

Tabitha R. Chigwada[†] and Reuben H. Simoyi*

Department of Chemistry, Portland State University, Portland, Oregon 97207-0751

Received: September 24, 2004; In Final Form: November 19, 2004

The kinetics of the oxidation of a substituted thiourea, trimethylthiourea (TMTU), by chlorite have been studied in slightly acidic media. The reaction is much faster than the comparable oxidation of the unsubstituted thiourea by chlorite. The stoichiometry of the reaction was experimentally deduced to be $2ClO_2^- + Me_2N(NHMe)C{=}S + H_2O \rightarrow 2Cl^- + Me_2N(NHMe)C{=}O + SO_4^{2-} + 2H^+$. In excess chlorite conditions, chlorine dioxide is formed after a short induction period. The oxidation of TMTU occurs in two phases. It starts initially with S-oxygenation of the sulfur center to yield the sulfinic acid, which then reacts in the second phase predominantly through an initial hydrolysis to produce trimethylurea and the sulfoxylate anion. The sulfoxylate anion is a highly reducing species which is rapidly oxidized to sulfate. The sulfinic and sulfonic acids of TMTU exists in the form of zwitterionic species that are stable in acidic environments and rapidly decompose in basic environments. The rate of oxidation of the sulfonic acid is determined by its rate of hydrolysis, which is inhibited by acid. The direct reaction of chlorine dioxide and TMTU is autocatalytic and also inhibited by acid. It commences with the initial formation of an adduct of the radical chlorine dioxide species with the electron-rich sulfur center of the thiocarbamide followed by reaction of the adduct with another chlorine dioxide molecule and subsequent hydrolysis to yield chlorite and a sulfenic acid. The bimolecular rate constant for the reaction of chlorine dioxide and TMTU was experimentally determined as $16 \pm 3.0\ M^{-1}\ s^{-1}$ at pH 1.00.

Introduction

We recently established a series of studies designed to elucidate the kinetics and mechanisms of the oxidation of thio compounds by oxyhalogen ions.[1] The primary aim of this series of experiments is to elucidate the mechanisms of the recently discovered chemical oscillatory systems that involve oxyhalogen−sulfur chemistry.[2] Most of the chemical oscillators in this subset are of the simple two-component types, but their mechanisms have been extremely elusive. In contrast with the well-known oxyhalogen oscillators such as the Belousov−Zhabotinsky and Bray reactions,[3,4] in which the nonlinearity in the kinetics is derived from the oxyhalogen chemistry subset,[5] the two-component oxyhalogen−sulfur oscillators can derive their nonlinear behavior from the sulfur chemistry subset as well. The simple chlorite−thiourea oscillator, for example, has shown a wide range of nonlinear behavior that rivals that from the venerable BZ system.[6] Some of the exotic dynamics derived from this supposedly simple system include homoclinic chaos in a continuously stirred tank reactor, CSTR.[7] No other chemical system has displayed such complex dynamics. A complete understanding of this chemical oscillator is possible only if the mechanism of the oxidation of thiourea by chlorite is known in detail.

One unique feature of the chlorite−thiourea reaction system is the generation of symmetry-breaking bifurcations in unstirred reaction systems.[8] Previous studies of the generation of lateral instabilities in the form of traveling waves had implicated cubic autocatalysis as a stringent prerequisite.[9] The chlorite−thiourea system generates traveling waves of acid, chlorine dioxide, and sulfate fronts from a point of initial perturbation.[10−12] Our studies on the mechanism of this reaction had only deduced quadratic autocatalysis.[13] It had been conjectured that the additional mechanism needed to fuel these instabilities could be convective, but no-one is certain, yet. Such pattern formation and symmetry-breaking bifurcations have now taken on a new significance since they could lead to a better understanding of asymmetric cell differentiation and the chemical basis of morphogenesis.[14]

Studies into the generic oxidation mechanisms by chlorite have suggested that there is an inherent instability built into the chlorite anion on the basis of the interactions of the reactive oxychlorine species that are generated during its reduction.[15] Other studies have implicated interfacial effects as being responsible for the some of the experimentally observed stochasticities generated in most reactions that involve chlorite.[16] At the same time, it was acknowledged that oxidations of organosulfur compounds, and, especially thiocarbamides, in themselves, can present nonlinearities on the basis of extensive sulfur−sulfur disproportionations and polymerizations. Indeed, the combination of the chlorite ion and any sulfur species invariably produces exotic dynamics in the form of clock reaction behavior, oligooscillations and oscillatory behavior in both batch and CSTR environments.[17] An attempt to generalize these reaction systems failed because each chlorite-sulfur compound reaction system seems to present a unique reactivity. Each reaction system has to be studied on its own.

This feature of the diversity in oxidation mechanisms of closely related sulfur compounds has been observed in biological chemistry.[18] Thioureas are known toxins, and substituted

* Corresponding author.
[†] Permanent address: Department of Chemistry, West Virginia University, Morgantown, WV 26506-6045.

10.1021/jp045650u CCC: $30.25
Published on Web 01/26/2005

thioureas are known to exhibit a number of pharmacological effects in toxicity and metabolic effects.[19] The main in vivo transformations of thioureas are oxidative, especially S-oxygenation in which there is successive addition of oxygen atoms on the sulfur atom until it is oxidatively saturated and cleaves off the parent compound as sulfate[20] or stays on as the sulfonic acid for organosulfur compounds with a β-amino group.[21,22] Generally, the oxidation of thioureas generates genotoxic products, and thus the evaluation of the oxidation mechanisms of thioureas could have a predictive advantage in terms of toxicities. Subtle differences in substituted thioureas can impart vastly different degrees of toxicity.[19,23,24]

We are revisiting, in this manuscript, the oxidation of thioureas by chlorite in which we examine the methyl-substituted thiourea: trimethylthiourea. Our interest in this series of compounds is two-fold. The first involves the varied and different metabolic effects observed with thiourea and dimethythiourea.[25,26] Thiourea is a strong goitrogenic and its antithyroid activity leads to a disruption of pituitary-thyroid hormonal regulatory system.[27] Dimethylthiourea, on the other hand, is one of the most efficient scavengers of reactive oxygen species in vitro and reduces oxidative injury in many biological systems. The assumption is that all metabolic processes involving these compounds are oxidative, and so their oxidative mechanisms as well as their metabolites must be different despite their similarities. The second involves the vastly different spatial patterns obtained in chlorite-trimethylthiourea and chlorite-tetramethylthiourea systems.[6] While both systems appear to be bistable and autocatalytic, they differ greatly in the structures they generate in unstirred conditions. Our previous studies had concluded that the observed symmetry-breaking bifurcations are heavily dependent on the chemical kinetics and energetics of the oxidation reactions. Subsequent convective instabilities (thermocapillary and thermogravitational) are also strongly dependent on the mechanism of the reaction.[11]

Our previous studies had concentrated on the clock-reaction behavior of the parent chlorite−thiourea reaction to evaluate reaction kinetics and mechanism. In this mode, the reaction was studied in excess oxidant conditions in which chlorine dioxide was obtained as a product after the complete consumption of the substrate.[28] By assuming that the rate of oxidation of thiourea by chlorine dioxide was fast, one could assume that chlorine dioxide formation denoted complete consumption of thiourea and its oxidation intermediates. Thus, induction periods (before formation of chlorine dioxide) could be related to the rate of oxidation of thiourea. This simple approach could not work with TMTU because reaction of chlorine dioxide with TMTU was quite sluggish. We have resorted, then, to utilize a new approach that includes the spectrophotometric observation of the rate of consumption of the substrate which could be combined with the experimental observations of chlorine dioxide formation.

Experimental Section

Materials. The following analytical grade chemicals were used without purification: perchloric acid (72%), barium chloride, sodium chloride, sodium chlorite (Aldrich), sodium perchlorate, soluble starch (Fisher), and trimethylthiourea (TMTU) (TCI). Solutions were prepared using singly distilled water. Commercially available sodium chlorite varied in purity (78−88%) with the main impurities being chloride and carbonate. The sodium chlorite was recrystallized once from a water/ethanol mixture to bring the assay value to 95%. The recrystallized chlorite was standardized iodometrically by adding excess acidified potassium iodide and titrating liberated iodine against sodium thiosulfate with freshly prepared starch as an indicator. Chlorine dioxide was prepared by the method of oxidizing sodium chlorate in a sulfuric acid/oxalic acid mixture.[29] The stream was passed through a sodium carbonate solution before being collected in ice-cold water at 4° C at a pH of ∼3.5. Standardization of ClO_2 was also accomplished by iodometric techniques through addition of excess acidified potassium iodide and back-titrating the liberated iodine against standard sodium thiosulfate using the following stoichiometry:

$$2ClO_2 + 10I^- + 8H^+ \rightarrow 5I_2 + 2Cl^- + 4H_2O \quad \text{(R1)}$$

The results obtained were confirmed spectrophotometrically by using the absorptivity coefficient of ClO_2 of 1265 M^{-1} cm^{-1} at 360 nm.

Tests for Adventitious Metal Ion Catalysis. Water used for preparing reagent solutions was obtained from a Barnstead Sybron Corporation water purification unit capable of producing both distilled and deionized water (Nanopure). We utilized inductively-coupled plasma mass spectrometry (ICPMS) to quantitatively evaluate the concentrations of a number of metal ions in the water used for our reaction medium. ICPMS analysis showed negligible concentrations of iron, copper and silver and approximately 1.5 ppb of cadmium and 0.43 ppb in lead. The use of chelators to sequester metal ions gave kinetics and reaction dynamics indistinguishable from those run in distilled−deionized water.

Methods. All experiments were carried out at 25±0.5 °C (Neslab thermostat circulating bath) and an ionic strength of 1.0 M (sodium perchlorate). The ClO_2^-/ClO_2/TMTU reactions were monitored spectrophotometrically at $\lambda = 360$ nm so as to utilize the formation of chlorine dioxide as an indicator of the reaction's progress. Kinetic measurements were performed on a Hi-Tech Scientific double-mixing SF61-DX2 stopped-flow spectrophotometer. The data from the spectrophotometer were amplified and digitized via an Omega Engineering DAS-50/1 16-bit A/D board interfaced to a Pentium IV computer for storage and data analysis. Stoichiometric determinations were carried out by mixing various ratios of chlorite and TMTU in volumetric flasks and scanning them spectrophotometrically for formation of ClO_2 after an incubation period of up to 2 days. Qualitative analysis of the sulfate was performed through its precipitation as $BaSO_4$. For reaction run in excess chlorite conditions, the excess oxidizing power was evaluated by addition of excess acidified iodide, which was then titrated against standard thiosulfate.

Results

Stoichiometry. The stoichiometry was determined by a combination of spectrophotometric, titrimetric, and gravimetric techniques and was evaluated as an oxidant-to-reductant ratio of 2:1.

$$2ClO_2^- + Me_2N(NHMe)C{=}S + H_2O \rightarrow 2Cl^- + Me_2N(NHMe)C{=}O + SO_4^{2-} + 2H^+ \quad \text{(R2)}$$

Figure 1 shows three superimposed spectra; one for (a) TMTU ($\lambda_{max} = 216$ nm, $\epsilon = 15\,646$ M^{-1} cm^{-1}), (b) trimethylurea ($\epsilon = 1046$ M^{-1} cm^{-1} at $\lambda = 216$ nm), and the other for (c) chlorine dioxide ($\epsilon = 397$ M^{-1} cm^{-1} at $\lambda = 216$ nm). The peaks are widely separated enough so as not to interfere with each other. Chlorine dioxide has a very small absorptivity coefficient at 216 nm, but trimethylurea contributes significantly to the absorbance at 216 nm. Initial rate measurements at 216 nm were

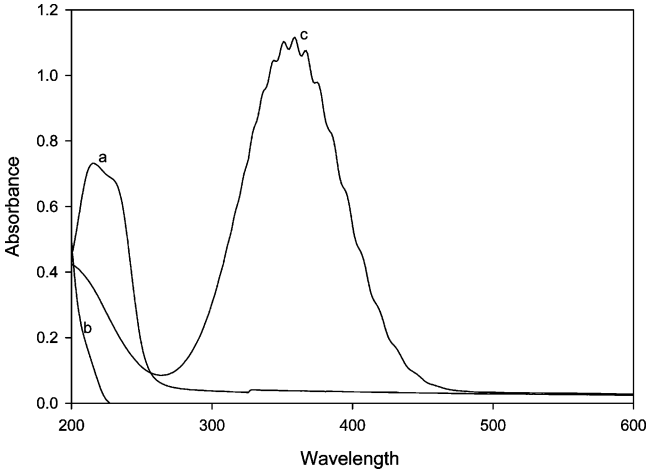

Figure 1. UV absorption spectrum of (a) 5.000×10^{-5} M TMTU, (b) 1×10^{-4} M trimethylurea (product) and (c) 8.8×10^{-4} M ClO_2 showing peaks at 216 and 360 nm. There is no interference from the substrate at 360 nm. At 216 nm, absorptivity coefficients are as follows: TMTU, 15, 646 M^{-1} cm^{-1}; TMU, 1046 M^{-1} cm^{-1}; ClO_2, 397 M^{-1} cm^{-1}.

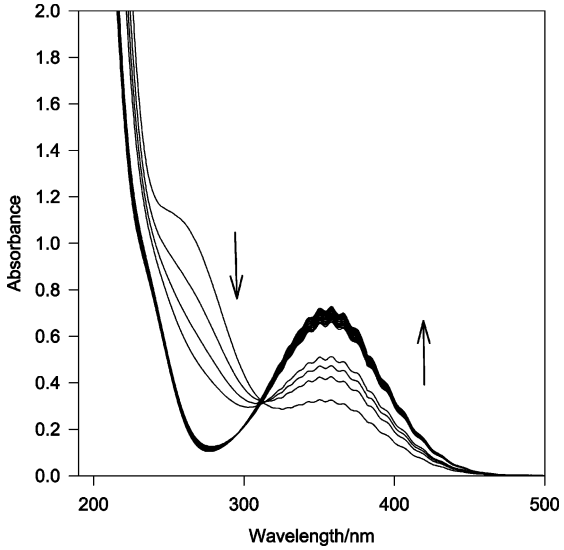

Figure 2. Absorbance scans of TMTU during oxidation by chlorite in aqueous acidic medium. Traces were collected every 30 s reaction time intervals. $[TMTU]_0 = 5 \times 10^{-4}$ M, $[ClO_2^-]_0 = 4 \times 10^{-3}$ M, and $[HClO_4]_0 = 0.1$ M.

able to deliver accurate data at the beginning of the reaction before concentrations of trimethylurea and chlorine dioxide accumulated.

The stoichiometric ratio needed for R2 was the highest amount of chlorite used for a fixed amount of TMTU that did not give chlorine dioxide as a product. Different ratios of chlorite and TMTU were mixed and left to incubate overnight. The reaction solutions were then spectrophotometrically examined the next morning for absorbance at 360 nm. These solutions were also qualitatively tested for sulfate formation by the addition of barium chloride. Those reaction mixtures that produced chlorine dioxide were then subjected to an iodometric titration to evaluate the excess oxidizing power left after all the TMTU had been consumed. By plotting thiosulfate volume needed vs chlorite used, the stoichiometry R2 was obtained by extrapolating to amount of chlorite needed for zero titer. The final complementary technique involved the data shown in Figure 3b. Chlorite concentrations were varied for a fixed TMTU concentration and the induction periods determined (time

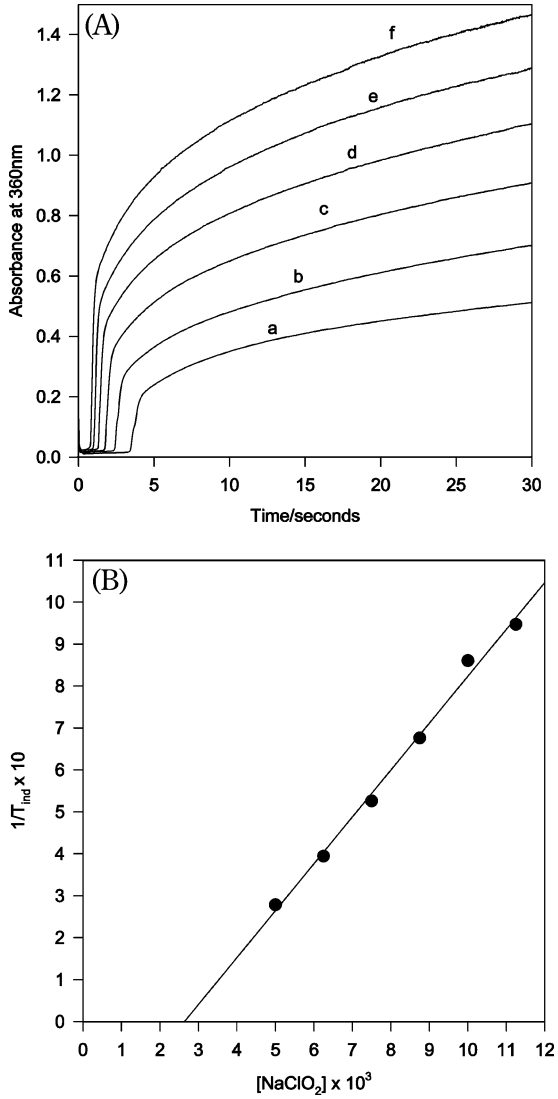

Figure 3. (A) Effect of chlorite on the absorbance at 360 nm. Concentration of chlorite is directly proportional to the amount of ClO_2 formed and inversely proportional to the induction period at fixed TMTU concentrations: $[TMTU]_0 = 1.25 \times 10^{-3}$ M, $[HClO_4]_0 = 0.125$ M, $[ClO_2^-]_0 =$ (a) 5.00×10^{-3}M, (b) 6.25×10^{-3} M, (c) 7.50×10^{-3} M, (d) 8.75×10^{-3} M, (e) $= 1.00 \times 10^{-2}$ M, (f) 1.125×10^{-2} M. (B) Plot of $1/_{T\,ind}$ vs $[ClO_2^-]$ using stoichiometric excess of chlorite, showing that an inverse relationship exists for a long range of chlorite concentrations. $[TMTU]_0 = 1.25 \times 10^{-3}$ M, $[HClO_4]_0 = 0.125$ M. The intercept value of $[ClO_2^-]_0 = 2.55 \times 10^{-3}$ M represents just enough ClO_2^- needed for consumption of TMTU with no excess ClO_2^- left to form ClO_2.

taken for the production of chlorine dioxide to commence). The intercept, where the induction period is ∞ ($1/T_{ind} = 0$; no chlorine dioxide formed), represents stoichiometry R2. Figure 3b shows that for a solution with 1.25×10^{-3} M TMTU; 2.55×10^{-3} M of chlorite was the intercept value where the induction period was ∞. This, then, also proved the 2:1 stoichiometry. Gravimetric analysis of sulfate as barium sulfate also proved that all the sulfur in TMTU ends up as sulfate. The trimethylurea product was identified by its UV spectrum.

Reaction Dynamics. At pH range of 1−3, the reaction displays a very short induction period followed by a rapid production of chlorine dioxide. Rapid scan spectra (see Figure 2) show an initial decrease in the TMTU peak at 216 nm with a delayed formation of the 360 nm peak. Figure 3a shows the 'clock' nature of this reaction. Initially, there is quiescence at

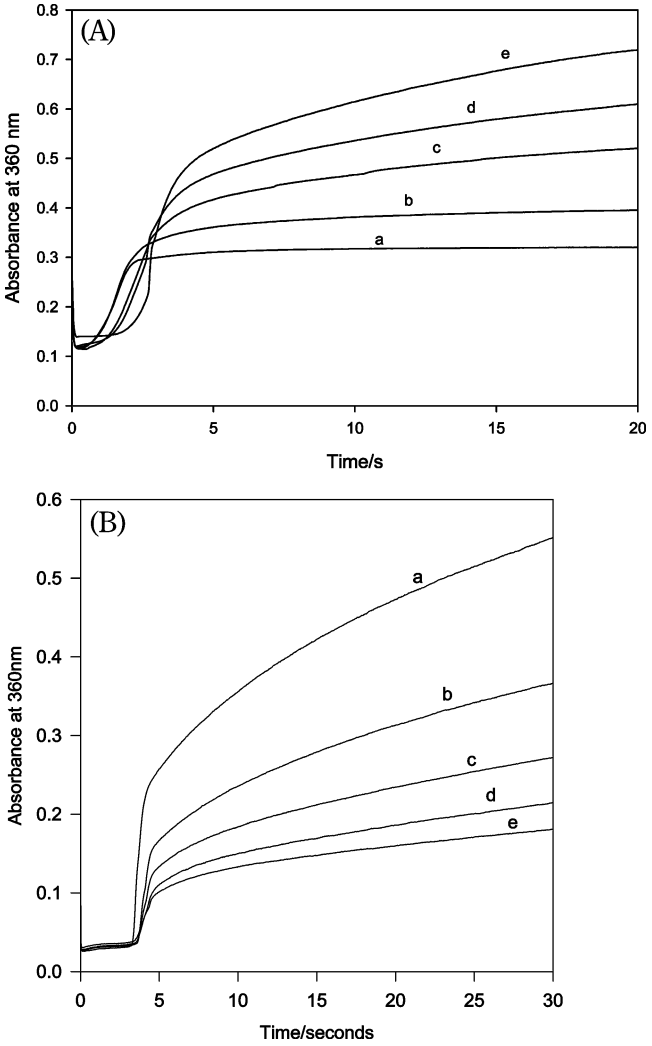

Figure 4. (A) Absorbance traces at 360 nm showing effect of low acid concentrations on the oxidation of TMTU by chlorite. In this case the induction period is not well defined but is slightly lengthened by increase in acid. The amount of chlorine dioxide formed is directly proportional to the amount of acid. $[TMTU]_0 = 1.25 \times 10^{-3}$ M, $[ClO_2^-]_0 = 5.00 \times 10^{-3}$M, $[HClO_4]_0 =$ (a) 0.005 M, (b) = 0.010 M, (c) 0.015 M, (d) 0.020 M, (e) 0.025 M. (B) Absorbance traces at 360 nm showing effect of high acid concentrations on the oxidation of TMTU by chlorite. In this case there is a well defined induction period which in not affected by the amount of acid. Concentration of acid is inversely proportional to the amount of chorine dioxide formed. $[TMTU]_0 = 1.25 \times 10^{-3}$ M, $[ClO_2^-]_0 = 5.00 \times 10^{-3}$M, $[HClO_4]_0 =$ (a) 0.1 M, (b) 0.2 M, (c) 0.3 M, (d) 0.4 M, (e) 0.5 M.

360 nm before chlorine dioxide is formed. This quiescent induction period's length is determined by initial reactant concentrations. In Figure 3a the only variable was initial chlorite concentrations. Higher chlorite concentrations gave shorter induction periods and a much more rapid rate of formation of chlorine dioxide. Figure 3b shows an inverse dependence between the induction period and chlorite concentrations. The induction period can be loosely related to the rate of reaction since the formation of chlorine dioxide should signal a specific event in the reaction's progress. Within these premises, one can assume that chlorite must be involved in the rate-determining step's rate law to the first power. In contrast, Figures 4a and b show a complex dependence of the reaction with acid. Figure 4a represents a low acid environment within the pH range of 1.6 to 2.3. In this environment, acid does not seem to affect the induction period, but does increase the rate and amount of

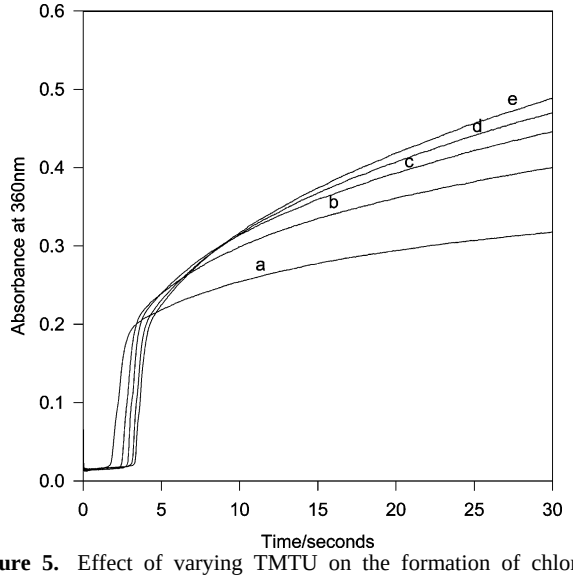

Figure 5. Effect of varying TMTU on the formation of chlorine dioxide. The amount of chlorine dioxide formed is directly proportional to the amount $[TMTU]_0$. $[ClO_2^-]_0 = 5.00 \times 10^{-3}$ M, $[HClO_4]_0 = 0.125$ M, $[TMTU]_0 =$ (a) 2.5×10^{-4} M, (b) 5.0×10^{-4} M, (c) 7.5×10^{-4}M, (d) 1.0×10^{-3} M, (e) 1.25×10^{-3} M.

chlorine dioxide formed after the induction period. The traces in Figure 4b were taken within the pH range of 0.7 and 1. Although acid still does not affect the induction period it now stunts the formation of chlorine dioxide after the induction period. The effect of TMTU observed in Figure 5 is expected: a lengthening of induction period with increase in TMTU at fixed ClO_2^- concentrations and an increase in rate and amount of chlorine dioxide. If production of chlorine dioxide signifies a specific progress in the oxidation of TMTU, this position will need a longer time to attain for a fixed amount of the oxidant, chlorite.

Consumption of TMTU. The reaction can be followed spectrophotometrically by monitoring the absorbance peak of TMTU at 216 nm. The product of the reaction, trimethylurea has a substantial absorbance at 216 nm (see Figure 1) and thus data such as those shown in Figure 6a are only used for the evaluation of reaction rates at the beginning of the reaction before other trimethylthiourea intermediates and chlorine dioxide start to assert themselves. The observed acid effects are also dependent on acid strength. Figure 6a shows that in high acid environments there is a monotonic decay in absorbance observed at 216 nm while in low acid (Figure 6b) the decay approaches a sigmoidal autocatalytic shape. The reaction appears to occur in two stages: an initial simple decay (high acid) followed by an autocatalytic decay (see Figure 6a trace a). However, the absorbance observed about 20 s into the reaction is dominated by trimethylthiourea oxo-acids and other species. It is no longer possible to attribute the absorbance to a single dominant species. Some of the absorbance contributions observed at this wavelength arise from the oxy-chlorine species as well (refer to Figure 1). Figure 7a shows the effect of chlorite at 216 nm. While chlorite appears to catalyze the initial stages of the reaction, the later stages of the reaction appear confusing. The baseline final absorbance observed is directly proportional to the initial chlorite concentrations, thus lending credence to the fact that oxy-chlorine species have substantial contributions to the absorbance observed at 216 nm. The criss-crossing of the absorbance traces is due to the fact that higher chlorite concentrations start with higher initial absorbances, and since chlorite catalyzes the reaction, these higher absorbance traces

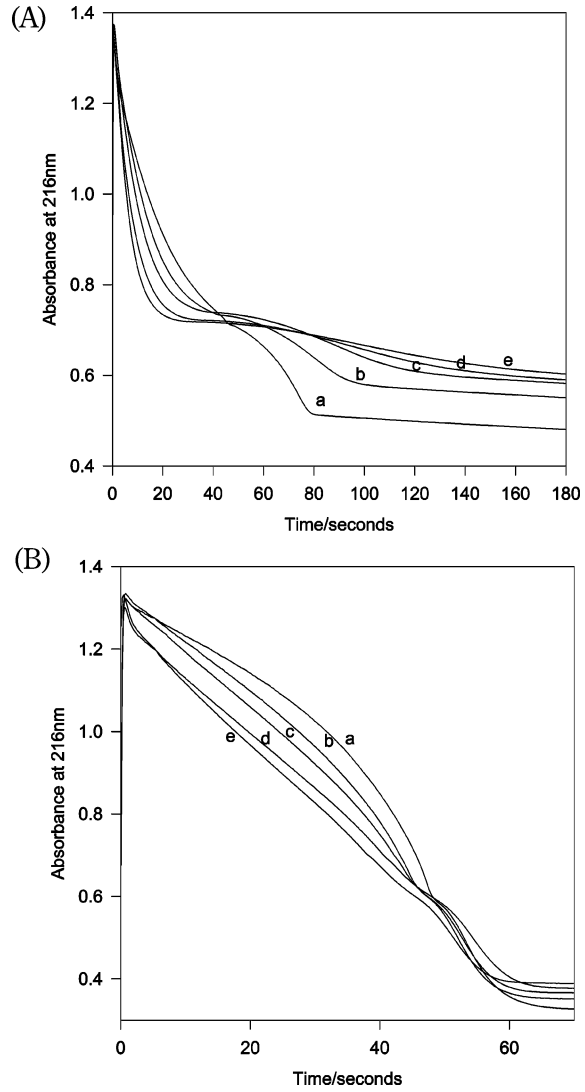

Figure 6. (A) Effect of acid on the depletion of TMTU in its oxidation by chlorite monitored at 216 nm. The reaction displays two-stage kinetics at lower acid concentrations. $[TMTU]_0 = 7.5 \times 10^{-5}$ M, $[ClO_2^-]_0 = 5.00 \times 10^{-4}$M, $[HClO_4]_0 =$ (a) 0.1 M, (b) 0.2 M, (c) 0.3 M, (d) 0.4 M, (e) 0.5 M. (B) Effect of acid on the depletion of TMTU in its oxidation by chlorite monitored at 216 nm. $[TMTU]_0 = 7.5 \times 10^{-5}$ M, $[ClO_2^-]_0 = 5.00 \times 10^{-4}$M, $[HClO_4]_0 =$ (a) 0.005 M, (b) 0.010 M, (c) 0.015 M, (d) 0.020 M, (e) 0.025 M.

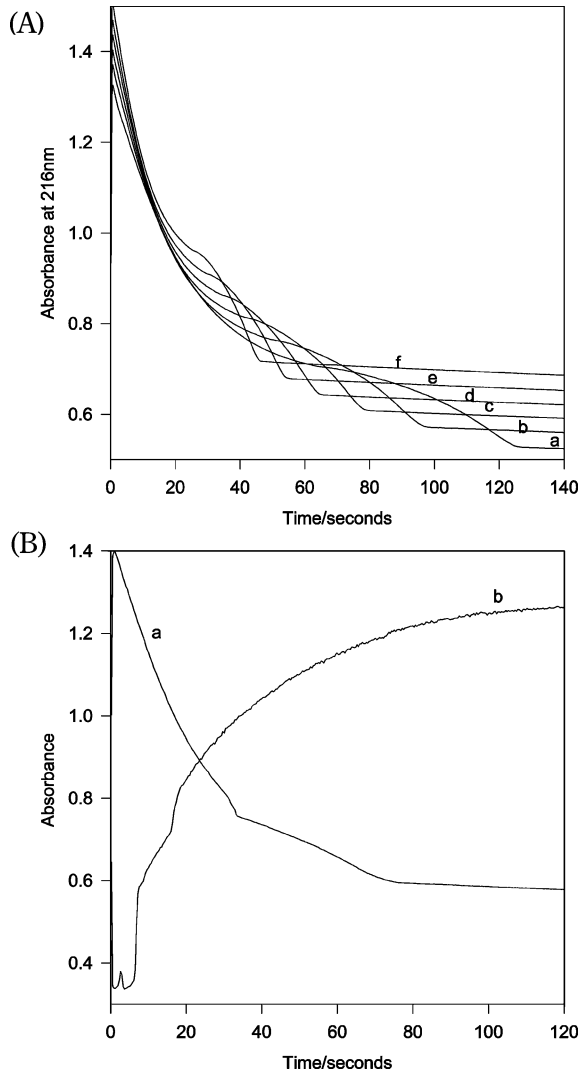

Figure 7. (A) Effect of chlorite on the depletion of TMTU in its oxidation by chlorite monitored at 216 nm. The data displays two-stage kinetics. The products of the TMTU oxidation give residual absorbance as can be seen in the absorbance−time data. $[TMTU]_0 = 7.5 \times 10^{-5}$ M, $[HClO_4]_0 = 0.125$ M, $[ClO_2^-]_0 =$ (a) 5.0×10^{-4} M, (b) 6.0×10^{-4} M, (c) 7.0×10^{-4} M, (d) 8.0×10^{-4} M, (e) 9.0×10^{-4} M, (f) 1.0×10^{-3} M. (B) Two traces superimposed at (a) 216 nm and (b) 360 nm. $[ClO_2^-]_0 = 5.00 \times 10^{-4}$M, $[TMTU]_0 = 5.0 \times 10^{-5}$ M, $[HClO_4]_0 = 0.125$ M.

will have to cross those traces at lower chlorite concentrations. The catalytic effect of chlorite is evident by noting the time taken for a final absorbance reading to be attained, and not by the value of the absolute reading itself. For example, final absorbance is reached in 42 s for an initial chlorite concentration of 0.001 M, while the reaction needs 125 s with 0.0005 M chlorite. An attempt was made, in Figure 7b to superimpose traces at 360 nm and at 216 nm. The absorbance readings at 360 nm had to be magnified 5× to fit on the same scale as those at 216 nm. In Figure 7b, one notices that chlorine dioxide production commences before the end of the first stage of the reaction. This is possible if reactions of chlorine dioxide with TMTU and its intermediates are slow enough to allow their coexistence. The data in Figures 8a and b are important in interpretation of the absorbance spectra. Due to the very high absorptivity coefficient of TMTU at 216 nm, only micromolar quantities are needed for optical density analysis. Thus in all the traces shown, oxidant-to-reductant ratio, $R = [ClO_2^-]_0/[TMTU]_0$ is very high and lies between 4.0 and 20. All TMTU will be quantitatively converted to the urea analogue with an ever-increasing final baseline absorbance as is observed in Figure 8a. A plot of the final absorbance vs initial TMTU concentrations will give a straight line with a positive intercept which corresponds to the contributions in absorbance from all other species in the reaction mixture which are not from the trimethylurea product. These data were utilized further in the deduction of the stoichiometry and mechanism. The follow-up plot in Figure 8b shows a linear dependence on initial rate with TMTU as expected. The intercept of this plot was kinetically indistinguishable from zero.

Oxidations by Chlorine Dioxide. Oxidation reactions of chlorine dioxide are comparable in rate with those of chlorite. This renders chlorite−TMTU reactions complex and difficult to interpret because formation of chlorine dioxide does not imply that all the reducing species in the reaction medium have been completely oxidized. This is also evident in Figure 7b. In Figure 9 a series of traces are shown with varying chlorine dioxide concentrations. Each trace shows a sigmoidal autocatalytic trace

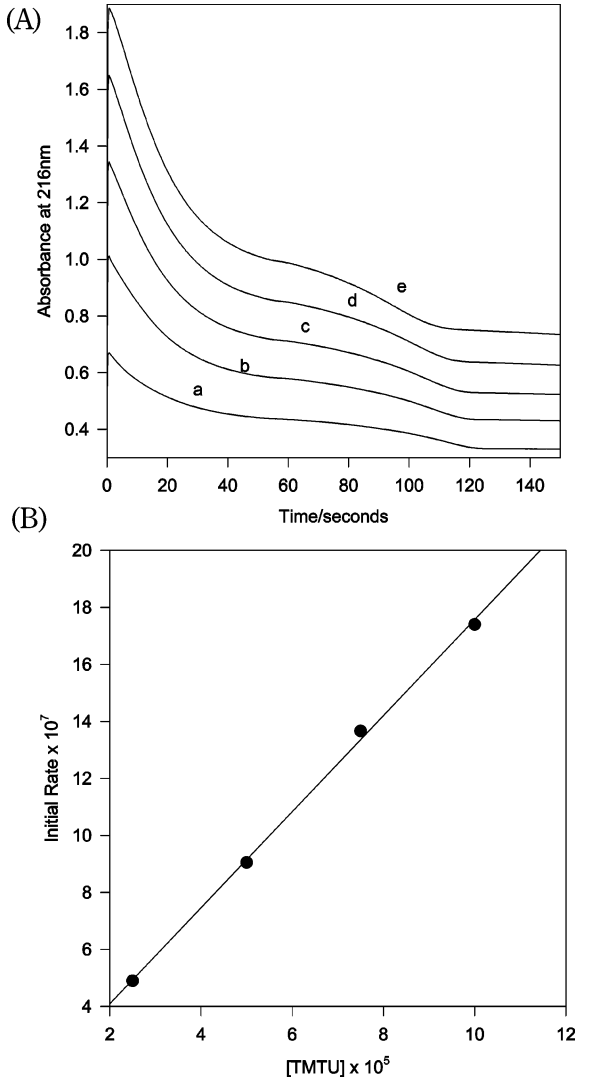

Figure 8. (A) Depletion of TMTU in its oxidation by chlorite. The data also displays two-stage kinetics. $[ClO_2^-]_0 = 5.00 \times 10^{-4}$M, $[HClO_4]_0 = 0.125$ M, $[TMTU]_0 =$ (a) 2.5×10^{-5} M, (b) 5.0×10^{-5} M, (c) 7.5×10^{-5} M, (d) 1.0×10^{-4} M, (e) 1.25×10^{-4} M. (B) Effect of initial TMTU concentration on the initial rate of consumption of TMTU. There is a solid linear dependence. $[ClO_2^-]_0 = 5.00 \times 10^{-4}$ M, $[HClO_4]_0 = 0.125$ M.

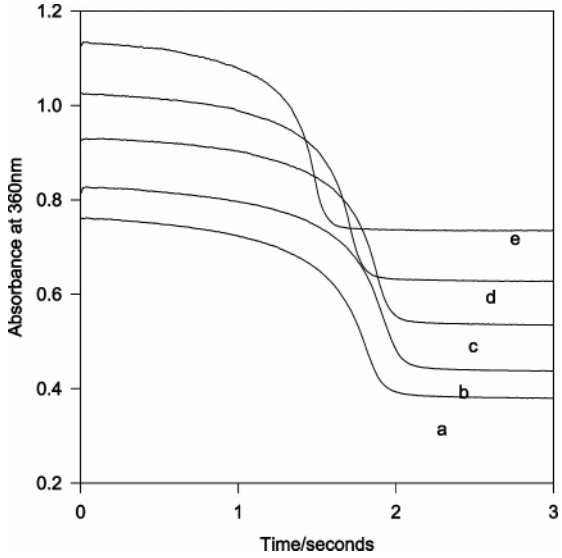

Figure 9. Effect of chlorine dioxide in the depletion of TMTU. Rate of depletion of TMTU increases with increase in chlorine dioxide concentrations. $[TMTU]_0 = 2.5 \times 10^{-4}$ M, $[HClO_4]_0 = 0.125$ M, $[ClO_2]_0 =$ (a) 7.0×10^{-4} M, (b) 8.0×10^{-4} M, (c) 9.0×10^{-4} M, (d) 1.0×10^{-3} M, (e) 1.1×10^{-3} M.

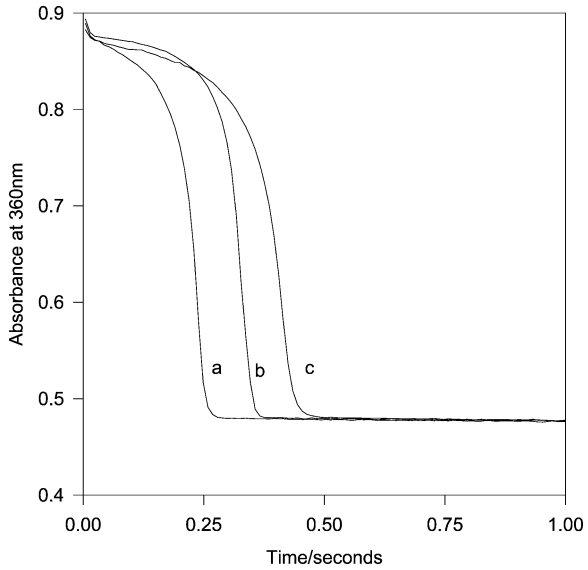

Figure 10. Effect of low acid concentrations on the oxidation of TMTU by chlorine dioxide. Rate of depletion of TMTU decreases with increase in acid concentrations. $[TMTU]_0 = 2.5 \times 10^{-4}$ M, $[ClO_2]_0 = 1.00 \times 10^{-3}$M, $[HClO_4]_0 =$ (a) 0.005 M, (b) 0.010 M, (c) 0.015 M.

with an ever-increasing rate of consumption of chlorine dioxide with time. Figure 10 shows that an increase in acid concentrations inhibits the reaction by lengthening the induction period before rapid oxidation commences. Previous studies had alluded to the fact that most chlorine dioxide oxidations proceed first through the formation of chlorite which then conducts the bulk of the oxidation.[30] The data shown in Figure 11 show the effect of very small amounts of chlorite on the rate of oxidation of TMTU by chlorine dioxide. Chlorite additions catalyze the reaction visibly, even at micromolar concentrations. Figure 11 also shows a control experimental run with no chlorite added. The parallel nature of the absorbance traces with varying concentrations of chlorite show that chlorite catalyses the reaction from $t = 0$ but is, in itself, not an autocatalytic species. Addition of chloride ions lengthens the induction period and inhibits the reaction (data not shown). Figures 12a and b show a series of experiments in which $[TMTU]_0 \gg [ClO_2]_0$. In Figure 12a the acid concentrations were fixed at 0.10 M. Just a monotonic decrease in chlorine dioxide concentrations is observed, which suggests that nonlinear autocatalytic catalysis is generated by the oxychlorine species and not from TMTU. A plot of initial rates of these traces vs $[TMTU]_0$ is linear, which indicates that the reaction of chlorine dioxide and TMTU is first order in [TMTU]. In Figure 12b, acid concentrations were elevated to 1.0 M and pseudo-first-order kinetics prevailed. The apparent rate constant evaluated for the various TMTU concentrations was invariant which indicates that at these acid concentrations the reaction became zero order in [TMTU]. From Figure 12a data, a bimolecular rate constant for the reaction of ClO_2 and TMTU of 16 $\forall$ 3.0 M^{-1} s^{-1} was evaluated.

Mechanism

While the reaction dynamics of the oxidation of TMTU by chlorite appear complex, they can easily be rationalized by two rapid protolytic reactions that involve the protonation of the

chlorite anion and the TMTU molecule. Acid concentrations of the reaction conditions will then determine the dominant and active species and the subsequent global dynamics observed. The important and confusing data that need to be rationalized are contained in Figures 4a,b and 6a,b. The observed dynamics appear to run counter to the expected acid catalysis observed with all oxyhalogen species.

$$ClO_2^- + H^+ \rightleftharpoons HClO_2;\ K_{a1}^{-1} \qquad (R3)$$

$$Me_2N(NHMe)C{=}S + H^+ \rightleftharpoons [Me_2N(NHMe)C{=}S{-}H]^+,\ ([TMTU{-}H]^+);\ K_b \qquad (R4)$$

From these two protonation reactions, four rate-determining step reactions can be derived in which the primary objective is the oxidation of TMTU by chlorite. The viability of these four reactions will depend on pH, and no conditions exist in which all four reactions will be simultaneously viable. At any pH conditions, not more than two of these reactions will dominate. Thus, it should be easy to evaluate rate constants without involving too many variables. The first intermediate, after a two-electron oxidation of TMTU is the sulfenic acid; $Me_2N(=NMe)C{-}SOH$, TMTUSOH. The one-electron oxidation of TMTU to produce thiyl radicals is mediated by one-electron metal ion oxidants such as Cu^{2+} and Fe^{3+}.[31,32] Since our reagent solutions were stripped of metal ions, we consider the dominant oxidation route to be through the sulfur-based oxo-acids which progressively proceed through sulfenic, sulfinic, and sulfonic acids before oxidative saturation of the sulfur center to eliminate sulfate. The following four reactions, R5−R8, will initiate the oxidation of TMTU:

$$TMTU + ClO_2^- \rightarrow TMTUSOH + OCl^-;\ k_1 \qquad (R5)$$

$$TMTU + HClO_2 \rightarrow TMTUSOH + HOCl;\ k_2 \qquad (R6)$$

$$[TMTU\text{-}H]^+ + ClO_2^- \rightarrow TMTUSOH + HOCl;\ k_3 \qquad (R7)$$

$$[TMTU\text{-}H]^+ + HClO_2 \rightarrow TMTUSOH + HOCl + H^+;\ k_4 \qquad (R8)$$

$$OCl^- + H^+ \rightleftharpoons HOCl \qquad (R9)$$

Low acid concentrations in Figures 4a and 6b will be dominated by reactions R5 and R6 while high acid concentrations in Figures 4b and 6a will be dominated by reactions R6 and R8. It will be difficult to find a balance where reaction R7 would contribute substantially, and even if this region is found, it should exist over a very short range in pH. By utilizing the standard mass balance equations with respect to Cl(III) species and TMTU species, the rate laws for the consumption of TMTU in Figures 6a and b can be derived.

$$[Cl(III)]_T = [ClO_2^-] + [HClO_2] \qquad (1)$$

$[Cl(III)]_T$ and $[TMTU]_T$ are the amounts of chlorite and TMTU

$$[TMTU]_T = [TMTU] + [TMTU\text{-}H]^+ \qquad (2)$$

added to the reaction solution before they partition into the protonated and unprotonated versions. At low acid environments,

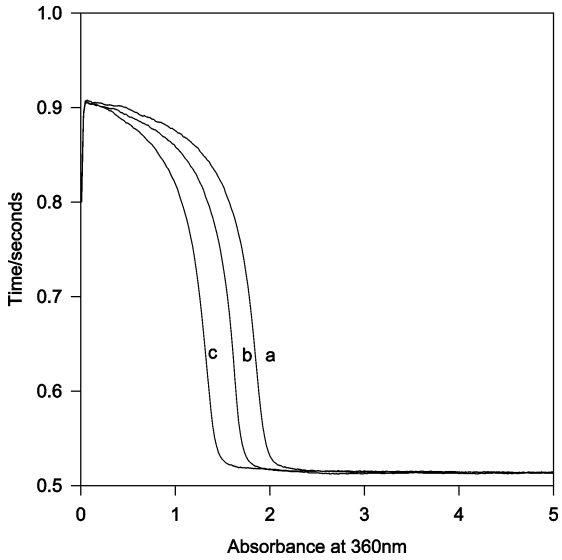

Figure 11. Effect of chlorite on the oxidation of TMTU by chlorine dioxide. $[TMTU]_0 = 2.5 \times 10^{-4}$ M, $[ClO_2]_0 = 1.00 \times 10^{-3}$M, $[HClO_4]_0 = 0.125$ M, $[ClO_2^-] =$ (a) 0.0 M, (b) 1.0×10^{-5} M, (c) 1.5×10^{-5} M.

the rate of consumption of TMTU will follow the following rate law:

$$\frac{-d[TMTU]}{dt} = \frac{[TMTU]_0[Cl(III)]_T}{1 + K_{a1}[H^+]}(k_1 + k_2K_{a1}[H^+]) \qquad (3)$$

We should then expect, in high acid environments, the following complex rate law in acid:

$$\frac{-d[TMTU]}{dt} = \frac{K_{a1}[H^+][Cl(III)][TMTU]_T}{(1 + K_{a1}[H^+])(1 + K_b[H^+])}(k_2 + k_4K_b[H^+]) \qquad (4)$$

The derivation of eq 4 assumes that reactions R5 and R7 will be negligible. In either case, one expects first-order kinetics in chlorite and TMTU. This is in agreement with our experimental data. The next issue is to rationalize the observed change in the consumption dynamics of TMTU as acid is increased. In low acid concentrations, Figure 6b shows a convex sigmoidal consumption profile that is indicative of autocatalysis while in Figure 6a, at higher acid concentrations the profile approaches the normal concave shape where standard mass action kinetics dominates. Autocatalysis in chlorite oxidations through HOCl has been reported repeatedly, and one expects this to be the case at low acid environments. All the oxidation pathways in R5−8 produce HOCl as a reactive and active intermediate. HOCl is a much more efficient and effective oxidant than chlorite. The remaining chlorite in the reaction medium reacts with HOCl to produce the asymmetric intermediate which was isotopically deduced by Taube and Dodgen:[33]

$$ClO_2^- + HOCl + H^+ \rightleftharpoons Cl_2O_2 + H_2O \qquad (R10)$$

Any further reduction of this intermediate will produce two molecules of HOCl, thus installing quadratic autocatalysis on the rate of consumption of TMTU.[15,34,35]

$$Cl_2O_2 + 2H^+ + 2e^- \rightarrow 2HOCl \qquad (R11)$$

The two-electron reductant could be TMTU or any of its metabolites that have not yet been oxidatively saturated to sulfate. Under these conditions that support autocatalysis, both

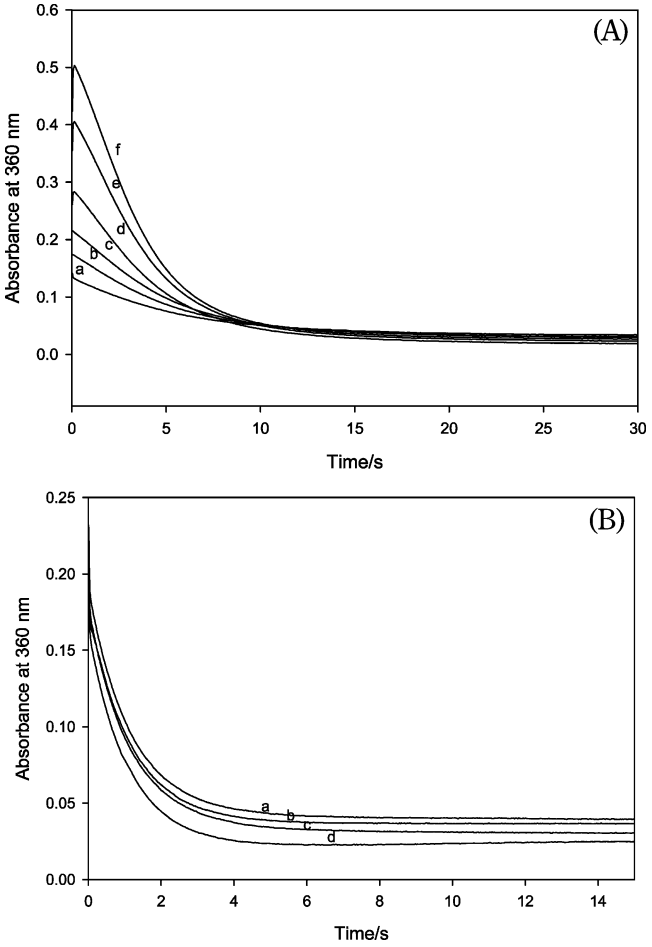

Figure 12. (A) Variation of chlorine dioxide in high excess of TMTU at intermediate acid concentrations. At 0.1 M acid concentrations, all Cl(III) species are in the chlorous acid form, but the TMTU is mostly unprotonated. $[TMTU]_0 = 0.01$ M, $[H^+]_0 = 0.10$ M, $[ClO_2]_0 =$ (a) 4.5×10^{-5} M, (b) 9.0×10^{-5} M, (c) 1.35×10^{-4} M, (d) 2.7×10^{-4} M, (e) 3.6×10^{-4} M, (f) 4.5×10^{-4} M. (B) Pseudo-first-order kinetics in high excess of TMTU and high acid concentrations. At 1.0 M acid concentrations both C(III) species and TMTU are protonated. $[ClO_2]_0$ = (a) 1.8×10^{-4} M, $[H^+]_0 = 1.0$ M, $[TMTU]_0 =$ (a) 0.0175 M, (b) 0.0185 M, (c) 0.0190 M, (d) 0.0195 M.

$HClO_2$ and ClO_2^- are active, with the major autocatalytic route coming from ClO_2^-. The protonated chlorous acid will not rapidly undergo reaction R10, which should be a composite 2-step process in which ClO_2^- initially reacts with HOCl followed by H^+ to release a water molecule. In high acid environments, however, the predominant species is $HClO_2$. The initial reagent ratios used in Figure 6a have an overwhelming excess of $HClO_2$ (ratio $R = 7$). This approaches pseudo-first order kinetics in which TMTU will be rapidly consumed before nonlinear behavior is allowed to asset itself. By assuming predominance of $HClO_2$, one can rewrite eq 4 as

$$\frac{-\mathrm{d}[TMTU]}{\mathrm{d}t} = \frac{[HClO_2][TMTU]_T}{(1 + K_b[H^+])}(k_2 + k_4K_b[H^+]) \quad (5)$$

If K_b is low, and we assume $[HClO_2] \gg [ClO_2^-]$, then eq 5 just simplifies to

$$-\mathrm{d}[TMTU]/\mathrm{d}t = k_2[Cl(III)]_T[TMTU]_T \quad (6)$$

where a reasonable value of k_2 can be evaluated in high acid concentrations (for example, Figure 6a, first phase of the reaction). Equation 5 clearly supports a standard concave shape with respect to consumption of TMTU. The specific acid dependence effect will be derived from the relative values of $[H^+]$, k_4, and K_b. However, for as long as $k_4 > k_2$, acid will not be inhibitory. It would have been inhibitory if reaction R7 was a major route of oxidation of TMTU. The removal of the effectiveness of reaction R5 by the increasing acidic conditions will bring about a visible change in the observed profile of the rate of consumption of TMTU as has been observed between Figures 6a and b. Experimentally, the catalytic effect of acid quickly saturates and subsequently inhibits in conditions of acid concentrations greater than 0.6 M, which implies that under these conditions only reaction R8 will be viable as reaction R6 loses its dominance.

Further Oxidation of TMTU. The sulfenic acid formed in the rate-determining steps, R5−R8, should be unstable and easily further oxidized to the more stable sulfinic and sulfonic acids in a series of irreversible, entropy-driven two-electron-transfer steps

$$TMTUSOH + HOCl \rightarrow TMTUSO_2H + H^+ + Cl^- \quad (R12)$$

$$TMTUSO_2H + HOCl \rightarrow TMTUSO_3H + H^+ + Cl^- \quad (R13)$$

In the absence of further oxidant, sulfenic acids are known to either dimerize through a condensation reaction with an unoxidized TMTU molecule or disproportionate into thiosulfinates.[36−38]

Formation of Products. Our current and previous studies have shown us that sulfonic acids, such as $TMTUSO_3H$ produced in reaction R13, are extremely stable and unreactive.[39−41] The major route to oxidation of sulfinic acids is through the cleavage of the C−S bond to release a highly labile and reducing species, HSO_2^- (see reaction R14) and the urea analogue of the thiourea compound.[42,43] The direct oxidation of the sulfinic acid to the sulfonic acid produces an inert intermediate that reacts only very slowly.[40] This stability has been reported, observed, and documented in atmospheric chemistry where the hydroxymethanesulfonic acid (bisulfite addition compound) is so stable that it is considered the sink for all anthropogenic sulfur dioxide emissions. Highly acidic environments, however, stabilize the aqueous form of the sulfonic acid much more than the sulfinic acid. The cleavage of the C−S bond in sulfinic acid is aided by the nucleophilic solvent molecules, R14 (water, in this case). The same applies for the sulfonic acid, R15. Reactions R14 and R15 are extremely rapid and facile in basic environments and are the most important steps in guanidylation.[44]

$$Me_2N(=NMe)C\text{-}SO_2H + Nu{:}\ (H_2O) \rightarrow Me_2N(NHMe)C{=}O + HSO_2^- + H^+ \quad (R14)$$

$$Me_2N(=NMe)C\text{-}SO_3H + Nu{:}\ (H_2O) \rightarrow Me_2N(NHMe)C{=}O + HSO_3^- + H^+ \quad (R15)$$

The sulfoxylate anion and the bisulfite are rapidly oxidized to sulfate, leaving the rate of hydrolysis of the oxo-acids (R14 and R15) as the rate-determining steps in the oxidation of sulfinic and sulfonic acids.

The zwitterionic forms of the sulfinic and sulfonic acids are known and shown below. The above zwitterionic structures have been proved in dimethylthiourea by the fact that in both sulfinic and sulfonic acids, the C−N bond lengths are equivalent (1.303 Å) and lie between the double bond and single bond lengths. All S−O bonds are also equivalent. Our previous studies have shown that the C−S bond in the zwitterionic thiourea dioxide (sulfinic acid) is much longer (1.880 Å) than the one expected

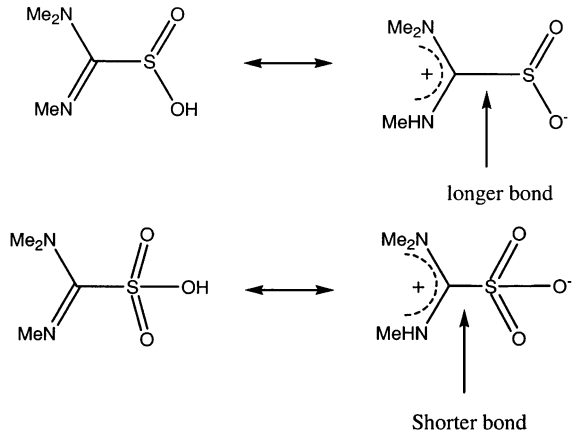

from merely adding covalent radii of C and S (1.79 Å) and that it is also longer than in the trioxide analogue (1.815 Å).[39] Thus, cleavage of the C−S bond is much easier at the sulfinic acid stage than at the sulfonic acid. In fact, most sulfonic acids are extremely inert in medium to low pH conditions.[40] The stability of the sulfonic acid at low pH can explain the observed retardation in chlorine dioxide formation with acid shown in Figure 4b. As has been quantified earlier, formation of chlorine dioxide is dependent upon the formation of HOCl; which in turn is dependent upon the rate of oxidation of the reducing substrates. The formation of a stable sulfonic acid in reaction R13 effectively stunts further oxidation and production of HOCl and thus starves the reaction that forms chlorine dioxide. Reactions R14 and R15 produce the readily oxidized sulfur species which increases the rate of formation of HOCl from chlorite. [Even though HOCl reacts faster with HSO_2^- and HSO_3^-, the most abundant species in the reaction medium is ClO_2^-, and it is mostly through ClO_2^- that these species will be oxidized]. The sequence of reaction steps after the formation of the sulfinic acid can best be represented by the schematic diagram shown below, where TMU is product trimethylurea.

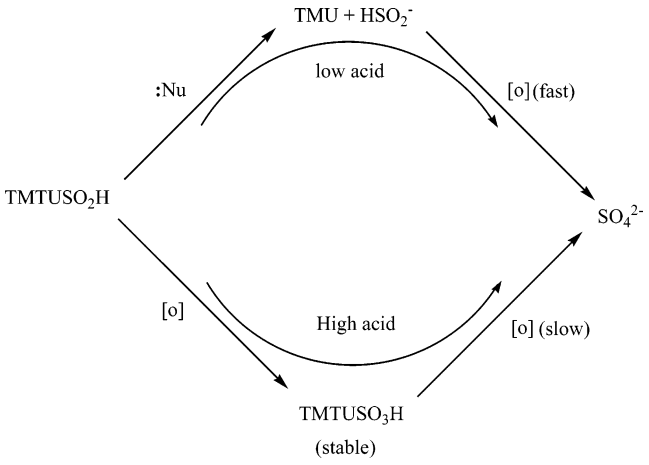

Further reaction of $TMTUSO_3H$ is very slow and first undergoes a hydrolysis to produce urea and bisulfite (reaction R15), which is then rapidly oxidized to sulfate.[40,41] The hydrolysis equilibrium, however, favors the sulfonic acid in high acid, and hence the reaction goes faster if the reaction solutions have been aged before oxidation rate is observed.[40] The reaction's duration is in the region of 200 s, which is insufficient time for incubation of the solutions to release bisulfite,[39,40]

Formation of Chlorine Dioxide. Chlorine dioxide is formed from the oxidation of chlorite by HOCl (primarily) and, to some extent, aqueous chlorine. In the absence of sufficient chlorite at the point where reactions R5 to R9 are producing HOCl, no chlorine dioxide will be formed. After reaction R10, chlorite will be rapidly oxidized by Cl_2O_2 to form chlorine dioxide:

$$Cl_2O_2 + ClO_2^- \rightarrow 2ClO_2 + Cl^- \qquad \text{(R16)}$$

Chlorine can be formed by its reverse disproportionation reaction:[45]

$$HOCl + H^+ + Cl^- \rightleftharpoons Cl_2 + H_2O \qquad \text{(R17)}$$

Chlorine will then rapidly oxidize chlorite to form chlorine dioxide:

$$Cl_2 + 2ClO_2^- \rightarrow 2ClO_2 + 2Cl^- \qquad \text{(R18)}$$

Since both reactions R16 and R18 are fast, the rate of formation of chlorine dioxide (before factoring in its consumption) should be proportional to the rate of formation of HOCl (see above). The data in Figure 3a are easily justified on that premise: higher chlorite concentrations, through pure mass-action kinetics, will produce HOCl at a higher rate, and hence a shortening of the induction period and an increase in the rate of formation of HOCl after the induction period will be observed. An examination of the data in Figures 4b and 6a will show that, even though the rate and amount of chlorine dioxide formed is depressed by higher acid concentrations, the rate of consumption of TMTU is still catalyzed by acid in the initial stages but decelerated later in the reaction (examine traces a and b). The deceleration is due to the stability of the sulfonic acid in highly acidic environments such that its further oxidation is retarded by acid, resulting in a slowing down of the reaction after the formation of the sulfinic and sulfonic acids. Figure 7b is very important in estimating the position in time at which chlorine dioxide is formed. The total consumption of TMTU and its metabolites is not necessary for the formation of chlorine dioxide, as has been observed in a comparable study of the oxidation of thiourea by chlorite.[28]

Chlorine Dioxide Consumption. Data in Figures 9−11 show typical consumption kinetics of chlorine dioxide. In all these experiments initial concentrations of chlorine dioxide and TMTU are approximately equal. This enables features such as autocatalysis and autoinhibition to prevail, should they exist, instead of being masked by pseudo-first-order kinetics if $[TMTU]_0 \gg [ClO_2]_0$. The rapidly increasing rate of oxidation of chlorine dioxide implicates HOCl autocatalysis. Oxidation by chlorine dioxide is expected to proceed through chlorite, which will then unleash the well-known oxychlorine species, HOCl. Chlorine dioxide is a radical species and should oxidize by a one-electron process. Mechanistically, we expect the electron-rich sulfur center of the TMTU to attack the electron-poor chlorine center to form a loose adduct.Further reaction of this adduct with

$$Me_2N(NHMe)C{=}S + {}^{\bullet}ClO_2 \rightleftharpoons [Me_2N(NHMe)C{=}S\text{-}ClO_2] \qquad \text{(R19)}$$

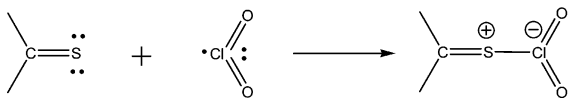

another ClO_2 molecule will produce the sulfenic acid and chlorous acid.

$$[Me_2N(NHMe)C{=}S\text{-}ClO_2] + ClO_2 + H_2O \rightarrow TMTUSOH + 2ClO_2^- + 2H^+ \quad (R20)$$

Each TMTU molecule will produce, in the initial stages, two molecules of chlorite, which is a better and more labile oxidizing agent than chlorine dioxide. Coupled with the acknowledged HOCl autocatalysis (R10 + R11), we expect an ever-increasing rate of reaction. Acid concentrations inhibit the reaction (see Figure 10) by shifting equilibrium of reaction R19 to the left due to protonation of TMTU and by the domination of $HClO_2$ over ClO_2^- among the products formed in reaction R20. Figure 11a shows that doping the reaction mixture with micromolar concentrations of chlorite rapidly accelerates the reaction, giving credence to the fact that reduction of ClO_2 goes through ClO_2^-.

Experimental Evaluation of Some Rate Constants. We can isolate one reaction from the rest out of the four possible rate-determining steps R5−R8. Figure 7a represents a perfect example of this isolation in the first stage of the reaction. One specific experimental run was performed at 1.00 M acid where we assumed dominance of reaction R6 and evaluated k_2 on the basis of rate eq 6. For statistical analysis and generation of error bars, other plots of initial rates vs chlorite were made and several values of k_2 were evaluated. The compilation gave a value of $k_2 = 1.58 \pm 0.3 \times 10^2\ M^{-1}\ s^{-1}$. Due to the approximation that most TMTU is unprotonated, this value of k_2 obtained represents an upper limit rate constant. The upper limit value of k_2 can be used to derive k_1 (the reaction between ClO_2^- and TMTU; reaction R5). Data in Figure 6a was then used together with rate eq 3 to derive a lower limit rate constant for k_1. This treatment gave a value of $k_1 = 52 \pm 9\ M^{-1}\ s^{-1}$. The inaccuracy observed in k_1 is derived from the change in kinetics as acid concentrations are increased. Acid dependence data from Figure 6b, with its sigmoidal decay kinetics are inadequate for initial rate determinations, and very high acid concentrations gave a saturation in rate with respect to acid concentrations. There was thus a very small window in which rate eq 3 was applicable. Figure 12a is another special figure produced just for the generation of a specific rate constant. By varying chlorine dioxide concentrations at constant acid and TMTU concentrations, a linear relationship is obtained from where the earlier-reported bimolecular rate constant of $16 \pm 3\ M^{-1}\ s^{-1}$ was derived. In Figure 12b the acid strength was increased to 1.00 M which gave, predominantly, $HClO_2$ as the Cl(III) species, and the protonated thiocarbamide. Under such extreme conditions pseudo-first-order kinetics could be obtained. The apparent rate constants from the semilog plots obtained from Figure 12b were invariant to TMTU concentrations. The deduced rate constant under these conditions was $10\ M^{-1}\ s^{-1}$.

Global Reaction Network. We have devised the full reaction scheme that encompasses reactions of both chlorite and chlorine dioxide into the set of reactions in Table 1. Not all 28 reactions are ever needed at the same time. For example, highly acidic conditions eliminated reactions M4 and M11−M14. The adopted reaction network has three rapid protolytic reactions, M1−M3 and three initiation reactions, M4−M6 (the fourth reaction between a protonated TMTU molecule and chlorite (reaction R7) was eliminated from the mechanism). HOCl is adopted in this mechanism as the dominant oxidizing species (reactions M7 to M10). The autocatalysis is accounted for in reactions M21, M23−M25.

A reasonable attempt to simulate this mechanism is heavily dependent on the knowledge of the kinetics parameters for reactions M17 and M18. There have been no studies so far on the kinetics and mechanisms of these hydrolysis reactions which appear to be general-base catalyzed. Without the requisite knowledge of these kinetics parameters, only the first phases of Figures 6a and 7a could be satisfactorily simulated. The observed autocatalytic decay of the sulfonic acid (second phase of the reaction in Figures 6a, 6b, and 7a) is derived from the expected rapid reaction between the sulfur leaving groups in reactions M17 and M18 with chlorine dioxide. Chlorine dioxide should rapidly form an adduct with bisulfite, which will then react with another chlorine dioxide molecule to form chlorite.

TABLE 1: The Complete Chlorite−Chlorine Dioxide−Trimethylthiourea Reaction Network

number	reaction
M1	$ClO_2^- + H^+ \rightleftharpoons HClO_2$; $K_{a1}^{-1} = 52.48$ M
M2	$TMTU + H^+ \rightleftharpoons TMTU{-}H^+$
M3	$OCl^- + H^+ \rightleftharpoons HOCl$; $K_{a2}^{-1} = 3.1 \times 10^7$ M
M4	$ClO_2^- + TMTU \rightarrow TMTUSOH + OCl^-$; $k_1 = 52\ M^{-1}\ s^{-1}$
M5	$HClO_2 + TMTU \rightarrow TMTUSOH + HOCl$; $k_2 = 1.58 \times 10^2\ M^{-1}\ s^{-1}$
M6	$TMTU{-}H^+ + HClO_2 \rightarrow TMTUSOH + HOCl + H^+$
M7	$TMTUSOH + HOCl \rightarrow TMTUSO_2H + Cl^- + H^+$
M8	$TMTUSO_2H + HOCl \rightarrow TMTUSO_3H + Cl^- + H^+$
M9	$TMTUSO_3H + HOCl \rightarrow TMU + SO_4^{2-} + Cl^- + 2H^+$
M10	$TMTU + HOCl \rightarrow TMTUSOH + Cl^- + H^+$
M11	$TMTUSOH + ClO_2^- \rightarrow TMTUSO_2H + OCl^-$
M12	$TMTUSO_2H + ClO_2^- \rightarrow TMTUSO_3H + OCl^-$
M13	$TMTUSO_3H + ClO_2^- + H_2O \rightarrow TMU + SO_4^{2-} + HOCl + H^+$
M14	$TMTUSOH + HClO_2 \rightarrow TMTUSO_2H + HOCl$
M15	$TMTUSO_2H + HClO_2 \rightarrow TMTUSO_3H + HOCl$
M16	$TMTUSO_3H + HClO_2 + H_2O \rightarrow TMU + SO_4^{2-} + HOCl + 2H^+$
M17	$TMTUSO_2H + H_2O \rightleftharpoons TMU + HSO_2^- + H^+$
M18	$TMTUSO_3H + H_2O \rightleftharpoons TMU + HSO_3^- + H^+$
M19	$HSO_2^- + HOCl \rightarrow HSO_3^- + Cl^- + H^+$; diffusion-controlled
M20	$HSO_3^- + HOCl \rightarrow SO_4^{2-} + Cl^- + 2H^+$; diffusion-controlled
M21	$ClO_2^- + HOCl + H^+ \rightleftharpoons Cl_2O_2 + H_2O$; $k_f = 1.01 \times 10^6\ M^{-2}\ s^{-1}$
M22	$Cl_2O_2 + ClO_2^- \rightarrow 2ClO_2 + Cl^-$
M23	$Cl_2O_2 + TMTU + H_2O \rightarrow TMTUSOH + 2HOCl$
M24	$Cl_2O_2 + TMTUSOH + H_2O$ 6 $TMTUSO_2H + 2HOCl$
M25	$Cl_2O_2 + TMTUSO_2H + H_2O$ 6 $TMTUSO_3H + 2HOCl$
M26	$2ClO_2 + TMTU + H_2O$ 6 $TMTUSOH + 2HClO_2$; $k_f = 16\ M^{-1}\ s^{-1}$
M27	$2ClO_2 + TMTUSOH + H_2O$ 6 $TMTUSO_2H + 2HClO_2$
M28	$2ClO_2 + TMTUSO_2H + H_2O$ 6 $TMTUSO_3H + 2HClO_2$

$$ClO_2 + HSO_3^- \rightleftharpoons [O_2Cl\text{-}SO_3H^-]; \text{ rapid} \quad (R21)$$

$$[O_2Cl\text{-}SO_3H^-] + ClO_2 + H_2O \rightarrow SO_4^{2-} + 2ClO_2^- + 3H^+; \text{ fast} \quad (R22)$$

The rapid formation of chlorite accelerates the reaction. Adduct formation between radical ClO_2 species and electron-rich nucleophiles has been recently reported by Nagypal et al. on the reaction of chlorine dioxide with thiosulfate and tetrathionate.[46,47] These are very rapid reactions with rates of the R21-type reactions close to diffusion control. Although no similar studies have been reported with bisulfite, one would assume that R21 should also be extremely rapid.

Conclusion

Our studies, in this manuscript, have shown that the oxidation kinetics of TMTU by chlorite is more complex than a comparable oxidation of the unsubstituted thiourea.[28] TMTU reactions are much faster and possess a much more complex behavior with respect to acid. Most of the complexity lies in the reactivities of the most important metabolite of TMTU, the sulfinic acid. While it is easily oxidized to the sulfonic acid, that route quickly terminates as further reaction from that metabolite is very slow. What could be most important is the ease by which the C−S bond is cleaved in the sulfinic acid because in aerobic conditions, we expect a concomitant production of reactive oxygen species that might bring with them inadvertent toxicity.[42]

Acknowledgment. We would like to thank Alice Chanakira for running most of the UV spectra of the reactants, products, and intermediates (Figure 1) and subsequently evaluating the various absorptivity coefficients and stoichiometric ratios. This work was supported by Research Grant Numbers CHE 0137435, CHE 0341152, and CHE 0341769 from the National Science Foundation.

References and Notes

(1) Chinake, C. R.; Mambo, E.; Simoyi, R. H. *J. Phys. Chem.* **1994**, *98*, 2908−2916.
(2) Doona, C. J.; Doumbouya, S. I. *J. Phys. Chem.* **1994**, *98*, 513−517.
(3) Kolaranic, L.; Schmitz, G. *J. Chem. Soc., Faraday Trans.* **1992**, *88*, 2343−2349.
(4) Melichercik, M.; Olexova, A.; Treindl, L. *J. Mol. Catal., A* **1997**, *127*, 43−47.
(5) Noyes, R. M. *J. Am. Chem. Soc.* **1980**, *102*, 4644−4649.
(6) Chinake, C. R.; Simoyi, R. H. *J. Phys. Chem.* **1994**, *98*, 4012−4019.
(7) Doona, C. J.; Blittersdorf, R.; Schneider, F. W. *J. Phys. Chem.* **1993**, *97*, 7258−7263.
(8) Martincigh, B. S.; Simoyi, R. H. *J. Phys. Chem. A* **2002**, *106*, 482−489.
(9) Petrov, V.; Scott, S. K.; Showalter, K. *Philos. Trans. R. Soc. London, Ser. A* **1994**, *347*, 631−642.
(10) Martincigh, B. S.; Chinake, C. R.; Howes, T.; Simoyi, R. H. *Phys. Rev. E* **1997**, *55*, 7299−7303.
(11) Martincigh, B. S.; Hauser, M. J. B.; Simoyi, R. H. *Phys. Rev. E* **1995**, *52*, 6146−6153.
(12) Martincigh, B. S.; Simoyi, R. H. *Phys. Rev. E* **1995**, *52*, 1606−1613.
(13) Hauser, M. J. B.; Chinake, C. R.; Simoyi, R. H. *S. Afr. J. Chem.* **1995**, *48*, 135−141.
(14) Turing, A. M. *Trans. R. Soc. (London)* **1952**, *B327*, 37−72.
(15) Rabai, G.; Orban, M. *J. Phys. Chem.* **1993**, *97*, 5935−5939.
(16) Khan, A. H.; Higginson, W. C. E. *J. Chem. Soc., Dalton Trans.* **1981**, *12*, 2537−2543.
(17) Rabai, G.; Beck, M. T. *J. Chem. Soc., Dalton Trans.* **1985**, 1669−1672.
(18) Mizutani, T.; Suzuki, K. *Toxicol. Lett.* **1996**, *85*, 101−105.
(19) Scott, A. M.; Powell, G. M.; Upshall, D. G.; Curtis, C. G. *Environ. Health Perspect.* **1990**, *85*, 43−50.
(20) Poulsen, L. L.; Hyslop, R. M.; Ziegler, D. M. *Arch. Biochem. Biophys.* **1979**, *198*, 78−88.
(21) Chinake, C. R.; Simoyi, R. H. *J. Phys. Chem. B* **1998**, *102*, 10490−10497.
(22) Chinake, C. R.; Simoyi, R. H. *J. Phys. Chem. B* **1997**, *101*, 1207−1214.
(23) Hollinger, M. A.; Giri, S. N.; Hwang, F.; Budd, E. *Res. Commun. Chem. Pathol. Pharmacol.* **1974**, *8*, 319−326.
(24) Smith, R. L.; Williams, R. T. *J. Med. Pharm. Chem.* **1961**, *4*, 137−146.
(25) Beehler, C. J.; Ely, M. E.; Rutledge, K. S.; Simchuk, M. L.; Reiss, O. K.; Shanley, P. F.; Repine, J. E. *J. Lab. Clin. Med.* **1994**, *123*, 73−80.
(26) Beehler, C. J.; Simchuk, M. L.; McCord, J. M.; Repine, J. E. *J. Lab. Clin. Med.* **1992**, *119*, 508−513.
(27) Jirousek, L.; Soodak, M. *J. Pharmacol. Exp. Ther.* **1974**, *191*, 341−348.
(28) Epstein, I. R.; Kustin, K.; Simoyi, R. H. *J. Phys. Chem.* **1992**, *96*, 5852−5856.
(29) Brauer, G. *Handbook of Preparative Organic Chemistry*; Academic Press: New York, 1963; p 301.
(30) Darkwa, J.; Olojo, R.; Chikwana, E.; Simoyi, R. H. *J. Phys. Chem. A* **2004**, *108*, 5576−5587.
(31) Pecci, L.; Montefoschi, G.; Musci, G.; Cavallini, D. *Amino Acids* **1997**, *13*, 355−367.
(32) Jeitner, T. M.; Lawrence, D. A. *Toxicol. Sci.* **2001**, *63*, 57−64.
(33) Taube, H.; Dodgen, H. *J. Am. Chem. Soc.* **1949**, *71*, 3330−3336.
(34) Peintler, G.; Nagypal, I.; Epstein, I. R. *J. Phys. Chem.* **1990**, *94*, 2954−2958.
(35) Salem, M. A.; Chinake, C. R.; Simoyi, R. H. *J. Phys. Chem.* **1996**, *100*, 9377−9384.
(36) Capozzi G.; Modena, G. *The chemistry of the thiol group*, 5th ed.; Wiley-Interscience: New York, 1974; pp 791−796.
(37) Choi, J. S.; Yoon, N. M. *J. Org.Chem.* **1995**, *60*, 3266−3267.
(38) McKillop, A.; Koyuncu, D. *Tetrahedron Lett.* **1990**, *31*, 5007−5010.
(39) Makarov, S. V.; Mundoma, C.; Penn, J. H.; Petersen, J. L.; Svarovsky, S. A.; Simoyi, R. H. *Inorg. Chim. Acta* **1999**, *286*, 149−154.
(40) Makarov, S. V.; Mundoma, C.; Penn, J. H.; Svarovsky, S. A.; Simoyi, R. H. *J. Phys. Chem. A* **1998**, *102*, 6786−6792.
(41) Ojo, J. F.; Otoikhian, A.; Olojo, R.; Simoyi, R. H. *J. Phys. Chem. A* **2004**, *108*, 2457−2463.
(42) Makarov, S. V.; Mundoma, C.; Svarovsky, S. A.; Shi, X.; Gannett, P. M.; Simoyi, R. H. *Arch. Biochem. Biophys.* **1999**, *367*, 289−296.
(43) Svarovsky, S. A.; Simoyi, R. H.; Makarov, S. V. *J. Chem. Soc., Dalton Trans.* **2000**, 511−514.
(44) Maryanoff, C. A.; Stanzione, R. C.; Plampin, J. N.; Mills, J. E. *J. Org. Chem.* **1986**, *51*, 1882−1884.
(45) Kustin, K.; Eigen, M. *J. Am. Chem. Soc.* **1962**, *84*, 1355−1359.
(46) Horvath, A. K.; Nagypal, I.; Epstein, I. R. *J. Phys. Chem. A* **2003**, *107*, 10063−10068.
(47) Horvath, A. K.; Nagypal, I. *J. Phys. Chem. A* **1998**, *102*, 7267−7272.